

# Controlled nucleation and crystallization in $\text{Fe}_2\text{O}_3\text{--CaO--SiO}_2$ glass

YONG-KEUN LEE, SE-YOUNG CHOI

*Department of Ceramic Engineering, Yonsei University, Seoul, Korea*

For the first time controlled nucleation and crystallization were studied for  $40\text{Fe}_2\text{O}_3\text{--}20\text{CaO--}40\text{SiO}_2$  (wt %) glass which is useful as thermoseeds for hyperthermia of cancer. To investigate the crystallization mechanism of  $\text{Fe}_2\text{O}_3\text{--CaO--SiO}_2$  glass, the Avrami parameter and the activation energy for crystallization were measured by isothermal and non-isothermal processes using classical and differential thermal analysis techniques. Magnetite was the main crystal phase and the maximum nucleation and crystal growth temperatures were 700 and 1000 °C, respectively. The value of kinetic parameters such as the Avrami constant, the activation energy, and the frequency factor, determined using isothermal and non-isothermal processes showed excellent agreement. The slopes of the Kissinger, and Matusita and Sakka plots were almost parallel to each other, and, consequently, crystal growth is believed to occur on a fixed number of nuclei, the  $m$  values being considered to be the same as the  $n$  values. Using  $m=1.5$  and  $n=1.5$ , it was found that diffusion-controlled crystal growth with a constant number of nuclei occurred and these result are in excellent agreement with those determined by the classical technique.

## 1. Introduction

The nucleation and crystallization of glasses are important in understanding the stability of glasses in practical applications where the formation of nuclei and subsequent crystal growth must be avoided, and to prepare glass-ceramics with desired microstructures and properties by controlled nucleation and crystallization. Parameters that should be known for a glass for these applications are the nucleation and crystal growth rates, the activation energy and the dimensionality of crystal growth.

The classical technique [1,2] commonly used to determine the nucleation rate is heating the glass at a certain temperature for a selected period of time, to develop a number of nuclei within the glass. The glass is then heated to a higher temperature for a short time, where detectable crystals grow on these nuclei. Assuming that each crystal grows from a single nucleus and that no new nuclei form or dissolve during crystal growth, the number of nuclei per unit volume of the glass can be determined by counting the number of crystals in a given volume with either an optical or an electron microscope. The nucleation rate is determined by repeating the same procedure at various temperatures and times. The crystal growth rate can also be determined similarly.

Recently, it has been demonstrated [3–5] that the differential thermal analysis (DTA) technique can also be used as an alternative method to determine the nucleation temperature range and the temperature for maximum nucleation rate. The advantage of the DTA technique is that it requires much less time than that needed for the classical technique described above.

$\text{Fe}_2\text{O}_3\text{--CaO--SiO}_2$  glass composition was chosen for this study because it is useful as thermoseeds for hyperthermia of cancer [6,7]. The purpose of the present study was to investigate the crystallization mechanism of  $\text{Fe}_2\text{O}_3\text{--CaO--SiO}_2$  glass. For this purpose, the Avrami parameter and the activation energy for crystallization were measured by isothermal and non-isothermal processes using classical and DTA techniques.

## 2. Experimental procedure

### 2.1. Glass preparation

The glass-forming region in the  $\text{Fe}_2\text{O}_3\text{--CaO--SiO}_2$  system was previously reported [8], and the glass composition used in this study was  $40\text{Fe}_2\text{O}_3\text{--}20\text{CaO--}40\text{SiO}_2$  (wt %). The glass was prepared from reagent-grade  $\text{Fe}_2\text{O}_3$ ,  $\text{CaCO}_3$  (Yakuri, Japan), and  $\text{SiO}_2$  (Junsei, Japan). A 60 g batch was melted at 1550 °C for 2 h in a Pt–Rh10% crucible using a kanthal-super furnace. The melt was poured into a preheated copper mould ( $45 \times 70 \times 5 \text{ mm}^3$ ) and 3–4 mm thick glass was obtained by pressing; it was then slowly cooled to room temperature.

### 2.2. Isothermal process

#### 2.2.1. Classical technique

The glass samples were cut into pieces of  $10 \times 10 \times 3 \text{ mm}^3$  and polished with SiC paper (no. 1200) and alumina powder (0.05  $\mu\text{m}$ ) using distilled water. For fixing the nucleation and crystal growth temperature ranges, the glass transition temperature,

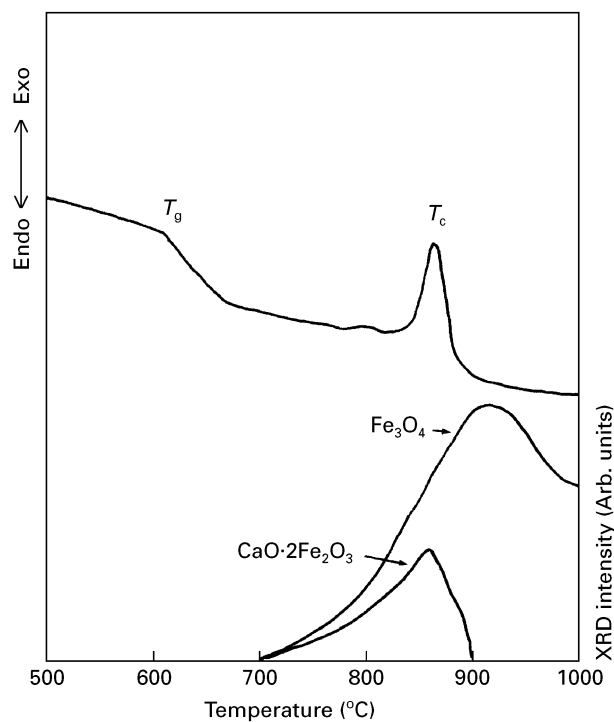
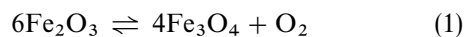


Figure 1 DTA curve at  $5 \text{ K min}^{-1}$  heating rate. The figure also shows the phases present as determined by XRD.

$T_g$ , and the exothermic temperature due to crystallization,  $T_c$ , were measured by DTA. Fig. 1 shows a typical DTA curve of  $40\text{Fe}_2\text{O}_3\text{-}20\text{CaO-}40\text{SiO}_2$  glass at a heating rate of  $5 \text{ K min}^{-1}$ , and also the amount of crystal phases determined by XRD. The main crystal phase was  $\text{Fe}_3\text{O}_4$  (magnetite), and  $\text{CaO}\cdot 2\text{Fe}_2\text{O}_3$  (iron ferrite) was also found below  $950^\circ\text{C}$ .

The oxidation–reduction reaction of iron can be written as [9]



Using  $\text{Fe}_2\text{O}_3$  as a raw material for the glass batch, part of the  $\text{Fe}_2\text{O}_3$  is reduced to  $\text{Fe}_3\text{O}_4$  during melting. Therefore, magnetite crystals can be obtained by heat treatment.

The number of nuclei was measured using a two-stage heat-treatment process. First the glasses were heated at  $5 \text{ K min}^{-1}$  to the nucleation temperature range between  $650$  and  $750^\circ\text{C}$  (intervals of  $25 \text{ K}$ ) for  $15\text{--}60 \text{ min}$  and then soaked for  $2 \text{ h}$  at  $1000^\circ\text{C}$  in order to grow nuclei to a detectable size.

After heat treatment, the specimens showed a change in colour from black to red only at the surface because of oxidation of  $\text{Fe}_3\text{O}_4$  into  $\text{Fe}_2\text{O}_3$  [9]. Therefore, after cooling to room temperature, the samples were ground to remove their surface layers and screened to  $< 50 \mu\text{m}$  and the number of crystallites (nuclei) was determined with TEM (JEM-400, Jeol, Japan).

The number of crystallites per unit volume,  $N_V$ , was calculated from [10]

$$N_V = (2/\pi)N_A Y/k(q) \quad (2)$$

where  $N_A$  is the number of particles per unit area,  $Y$  the mean value of the reciprocals of the measured

minor axis, and  $k(q)$  a correction factor dependent on the ratio,  $q$ , of the minor to major axes.

The size of crystallites was determined similarly. The nucleation temperature and time were fixed at  $700^\circ\text{C}$  and  $60 \text{ min}$ , respectively. The crystal growth temperatures ranged from  $950\text{--}1050^\circ\text{C}$  for intervals of  $25 \text{ K}$ . Crystal growth times lay between  $1$  and  $4 \text{ h}$ .

After calculating the crystal volume fraction from the size and number of crystallites per unit volume, the Avrami constant was obtained from the JMA equation [11]

$$X = 1 - \exp(-Kt^n) \quad (3)$$

where  $X$  is the crystal volume fraction,  $K$  the overall reaction rate,  $t$  the time, and  $n$  the Avrami constant. The  $\ln[-\ln(1-X)]$  versus  $\ln t$  plot should be a straight line, from the slope of which  $n$  can be obtained.

### 2.2.2. DTA technique

For the DTA measurements, the glass samples were ground and screened to  $< 50 \mu\text{m}$ . The glasses were heated at  $30 \text{ K min}^{-1}$  to the crystallization temperature range between  $750$  and  $1000^\circ\text{C}$  (at intervals of  $50 \text{ K}$ ) for  $10 \text{ min}$ . Then the Avrami constant and the activation energy were determined using the JMA equation as above.

### 2.3. Non-isothermal process

The activation energy and the dimensionality of crystal growth obtained by the non-isothermal process were determined using the DTA technique. The principle of the non-isothermal process is that the DTA exothermic peak temperature shifts to higher temperature with increasing heating rate. Then, the glass samples were heated at  $1.25$ ,  $2.5$ ,  $5$ ,  $10$ , and  $20 \text{ K min}^{-1}$ .

The value of the Avrami parameter or the order of the crystallization reaction,  $n$ , was determined from the Ozawa equation [12]

$$\left. \frac{d\{\ln[-\ln(1-X)]\}}{d\ln\phi} \right|_T = -n \quad (4)$$

where the volume fraction crystallized,  $X$ , is obtained at the same temperature,  $T$ , from a number of crystallization exotherms taken at different heating rates,  $\phi$ . The  $\ln[-\ln(1-X)]$  versus  $\ln\phi$  plot should be a straight line, from the slope of which  $n$  can be calculated.

The activation energy for crystallization was calculated primarily using the Kissinger equation [13]

$$\ln\left(\frac{\phi}{T_c^2}\right) = -\frac{E}{RT_c} + \text{const.} \quad (5)$$

where  $T_c$  is the temperature at the maximum of the crystallization peak and  $\phi$  is the DTA heating rate. A plot of  $\ln(\phi/T_c^2)$  versus  $1/T_c$  should be a straight line, whose slope yields the activation energy for crystallization,  $E$ .

TABLE I Values of  $n$  and  $m$  for various crystallization mechanisms

Mechanism		Three-dimensional (spherulites)		Two-dimensional (plates)		One-dimensional (needles)	
		$n$	$m$	$n$	$m$	$n$	$m$
Bulk nucleation with varying number of nuclei	Interface reaction	4	3	3	2	2	1
	Diffusion	2.5	1.5	2	1	1.5	0.5
Bulk nucleation with constant number of nuclei	Interface reaction	3	3	2	2	1	1
	Diffusion	1.5	1.5	1	1	0.5	0.5
Surface nucleation	Interface reaction	1	1	1	1	1	1
	Diffusion	0.5	0.5	0.5	0.5	0.5	0.5

Matusita and Sakka [14–16] have stated that the preceding non-isothermal equations can be used only when crystallization occurs on a fixed number of nuclei, i.e. the sample is well nucleated prior to crystal growth. If nucleation and crystal growth occur simultaneously, the slope of these plots depends also on the order of the crystallization reaction,  $n$ , and the value of  $E$  so determined will be much less than the true value. They have proposed a modified form of the Kissinger equation as

$$\ln\left(\frac{\phi^n}{T_c^2}\right) = -\frac{mE}{RT_c} + \text{const.} \quad (6)$$

where  $n$  is a constant known as the Avrami parameter, and  $m$  represents the dimensionality of crystal growth. The value of  $m$  is related to  $n$  as  $m = n$  when crystallization at different heating rates occurs on a fixed number of nuclei, i.e. the number of nuclei is constant during DTA runs at different heating rates, and  $m = n - 1$  when nucleation occurs during DTA and the number of nuclei in the glass is inversely proportional to the heating rate [17]. The values of  $n$  and  $m$  for various crystallization mechanisms obtained by Matusita and Komatsu [18] are shown in Table I.

### 3. Results and discussion

#### 3.1. Isothermal process by the classical technique

Fig. 2 shows a typical transmission electron micrograph. The electron round crystallites are magnetite. Figs 3 and 4 show the number of magnetite nuclei and the mean crystal diameters of magnetite as a function of nucleation and crystal growth time, respectively. The number of magnetite nuclei increased linearly with nucleation time and the maximum nucleation temperature was 700 °C. The size of magnetite increased linearly with the square root of crystal growth time and the maximum crystal growth temperature was 1000 °C. There are two mechanisms in crystal growth of glasses. One is the reaction between the glass melt and the crystal interface and the other is diffusion. The interface reaction is predominant, crystals grow with time, and crystals grow with the square root of time in the case where diffusion is predominant [19,20]. Therefore, it can be found that crystal growth in Fe<sub>2</sub>O<sub>3</sub>-CaO-SiO<sub>2</sub> glass is diffusion controlled.

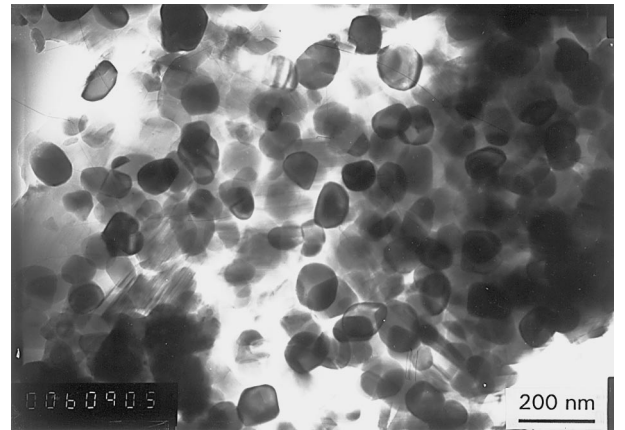


Figure 2 Transmission electron micrograph of the heat-treated sample (nucleation at 700 °C for 60 min and crystal growth at 1000 °C for 2 h).

From the crystal volume fractions of magnetite obtained by the classical technique, the Avrami plot of  $\ln[-\ln(1 - X)]$  versus  $\ln t$  from Equation 3 is represented in Fig. 5. The crystal volume fractions of magnetite increased linearly with heat-treatment time at each temperature and the Avrami constants determined from the slope of these plots are  $1.65 \pm 0.10$ .

#### 3.2. Isothermal process by the DTA technique

The Avrami plot obtained using the isothermal technique is represented in Fig. 6. As in Fig. 5, the crystal volume fractions increased linearly with heat-treatment time at each temperature and the Avrami constants determined from the slope of these plots are  $1.48 \pm 0.04$ . Fig. 7 exhibits the Arrhenius plot of the reaction rate,  $K$ , from the intercepts of Fig. 6. The reaction rates decreased linearly with the reciprocals of temperature and the activation energy and frequency factor determined from the slope and intercept, respectively, were 606.0 kJ mol<sup>-1</sup> and  $2.21 \times 10^{27} \text{ s}^{-1}$ .

#### 3.3. Non-isothermal process by the DTA technique

The DTA crystallization exotherms for various heating rates are shown in Fig. 8. The exothermic peaks

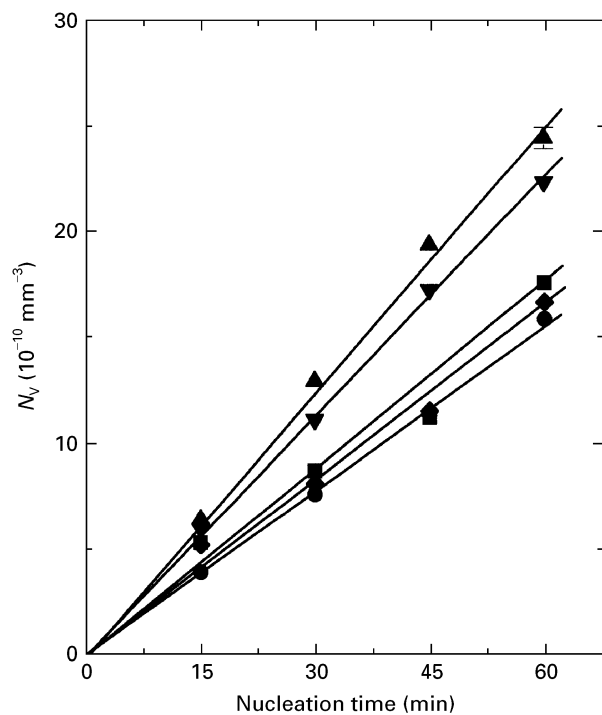


Figure 3 The number of magnetite nuclei as a function of nucleation time (crystal growth at 1000°C for 2 h) at: (●) 650°C, (■) 675°C, (▲) 700°C, (▼) 725°C, (◆) 750°C.

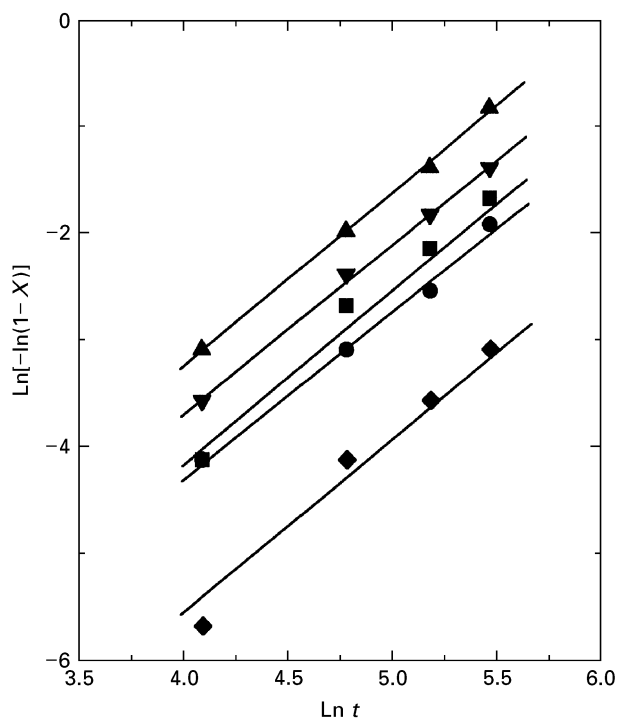


Figure 5 The Avrami plot of various temperatures determined by the isothermal process using the classical technique at: (●) 950°C, (■) 975°C, (▲) 1000°C, (▼) 1025°C, (◆) 1050°C.

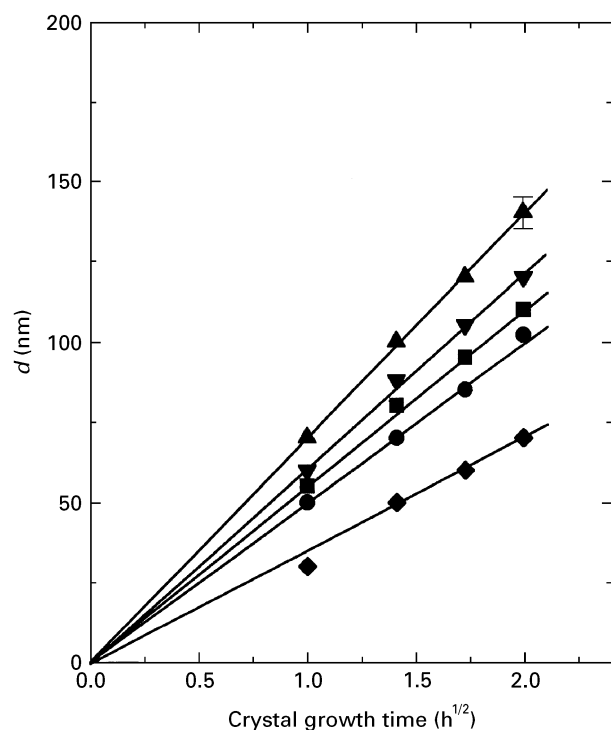


Figure 4 Crystal size of magnetite as a function of the square root of crystal growth time (nucleation at 700°C for 60 min) at: (●) 950°C, (■) 975°C, (▲) 1000°C, (▼) 1025°C, (◆) 1050°C.

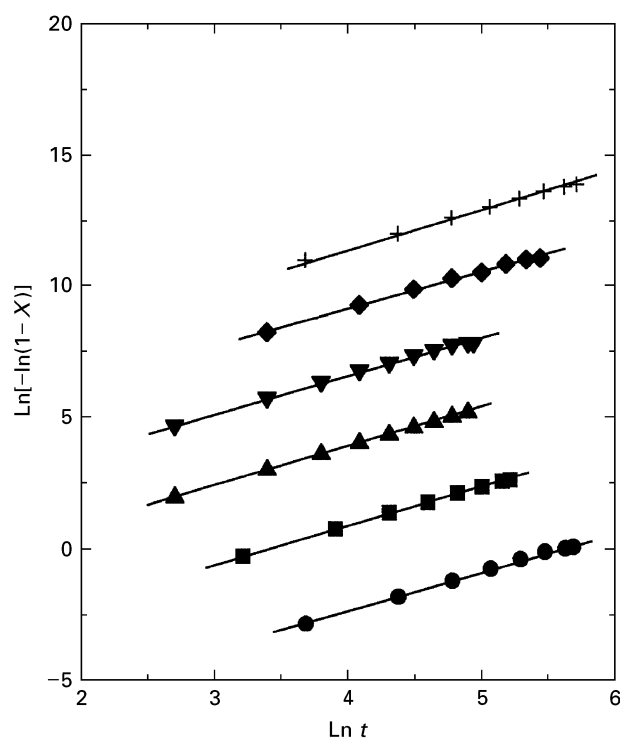


Figure 6 The Avrami plot of various temperatures determined by the isothermal process using the DTA technique at: (●) 750°C, (■) 800°C, (▲) 850°C, (▼) 900°C, (◆) 950°C, (+) 1000°C.

shift to higher temperatures with increasing heating rate and this result is in good agreement with previous reports [16, 21]. Fig. 8 exhibits sharp peaks, indicating that a bulk crystallization is predominant [22, 23].

Fig. 9 shows an Ozawa plot of  $\ln[-\ln(1-X)]$  versus  $\ln\phi$  from Equation 4, for heating rates of 1.25, 2.5, 5, 10, and 20  $\text{K min}^{-1}$ , where the crystal volume

fraction,  $X$ , was determined at 840°C. The value of  $n$  determined from the slope of this plot was 1.51.

The Kissinger, and Matusita and Sakka plots obtained from Equations 5 and 6, respectively, are shown in Fig. 10. The slopes of these plots are almost parallel to each other and, consequently,  $E$  is the same within experimental error. Therefore, crystal growth is

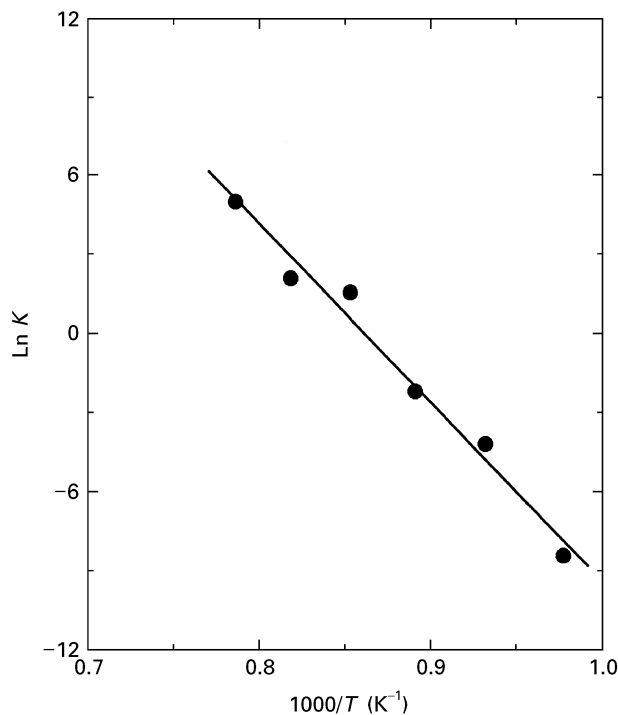


Figure 7 The arrhenius plot determined by the isothermal process using the DTA technique.

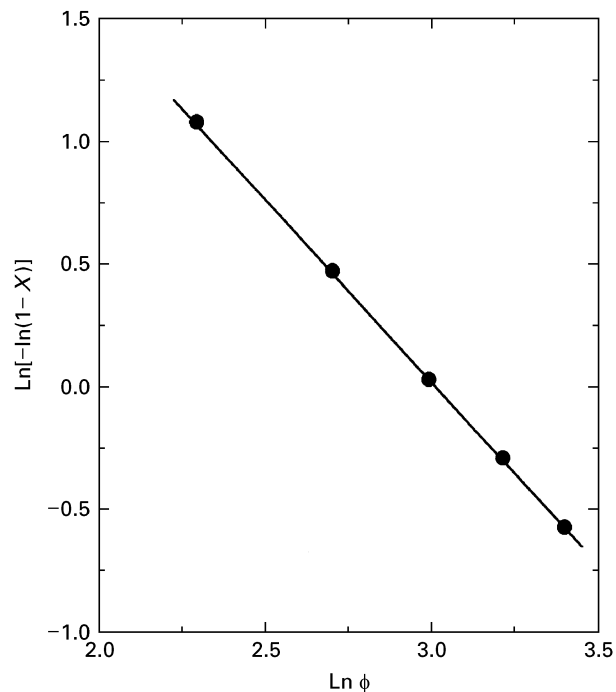


Figure 9 Ozawa plot of various heating rates determined by the non-isothermal process using the DTA technique.

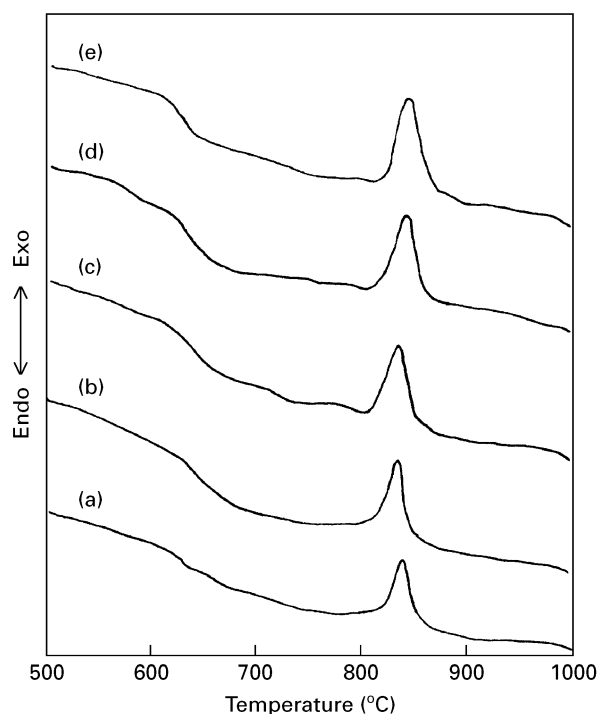


Figure 8 DTA exothermic peaks at various heating rates: (a) 1.25, (b) 2.5, (c) 5, (d) 10 and (e) 20 K min<sup>-1</sup>.

believed to occur on a fixed number of nuclei, and the  $m$  values are considered to be the same as the  $n$  values. Using  $m = 1.5$  and  $n = 1.5$ , it is found that the diffusion-controlled crystal growth with a constant number of nuclei occurred, and these results are in excellent agreement with those determined by the TEM technique.

The values of the activation energy and frequency factor determined from the slopes and intercepts of

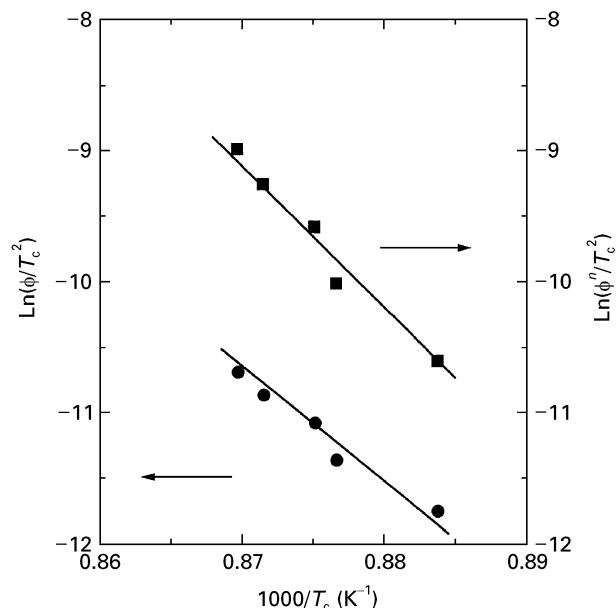


Figure 10 Plots of (●) the Kissinger and (■) the Matusita and Sakka equations at various heating rates determined by the isothermal process using the DTA technique.

these plots were  $636.4 \text{ kJ mol}^{-1}$  and  $2.69 \times 10^{27} \text{ s}^{-1}$ . The kinetic parameters for crystallization determined by isothermal and non-isothermal processes are shown in Table II. Avrami constants, the activation energies and the frequency factors are in excellent agreement, therefore isothermal and non-isothermal processes are both useful to investigate the crystallization mechanism of  $\text{Fe}_2\text{O}_3\text{-CaO-SiO}_2$  glass.

#### 4. Conclusion

For the first time, controlled nucleation and crystallization were studied for  $40\text{Fe}_2\text{O}_3\text{-}20\text{CaO-}40\text{SiO}_2$

TABLE II Comparison of kinetic parameters for crystallization determined by isothermal and non-isothermal processes

Parameters	Isothermal process		Non-isothermal process
	Classical technique	DTA technique	DTA technique
$n$	1.65	1.48	1.51
$E$ (kJ mol <sup>-1</sup> )	–	606.0	636.4
$v$ (s <sup>-1</sup> )	–	$2.21 \times 10^{27}$	$2.69 \times 10^{27}$

(wt %) glass, which is useful as thermoseeds for hyperthermia of tumor therapy. Magnetite was the main crystal phase and the maximum nucleation and crystal growth temperatures are 700 and 1000°C, respectively.

The DTA crystallization exothermic peaks shift to higher temperatures with increasing heating rate. The value of the kinetic parameters, such as the Avrami constant, the activation energy, and the frequency factor, determined using isothermal and non-isothermal processes, are excellent agreement. The slopes of the Kissinger, and Matusita and Sakka plots are almost parallel to each other and, consequently, crystal growth is believed to occur on a fixed number of nuclei, the  $m$  values being considered to be the same as the  $n$  values. Using  $m = 1.5$  and  $n = 1.5$ , it was found that the diffusion-controlled crystal growth with a constant number of nuclei occurred and these results are in excellent agreement with those determined by the classical technique.

## Acknowledgement

This research was financially supported by the Korea Science and Engineering Foundation under the contract 931-0800-013-1.

## References

1. P. F. JAMES, *Phys. Chem. Glasses* **15** (1974) 95.
2. E. D. ZANOTTO and A. GALHARDI, *J. Non-Cryst. Solids* **104** (1988) 73.
3. A. MOROTTA, in "Nucleation and Crystallization in Glasses" edited by J. H. Summons, D. R. Uhlmann and G. H. Beall (American Ceramic Society, Columbus, OH, 1982) p. 146.
4. C. S. RAY and D. E. DAY, *J. Am. Ceram. Soc.* **73** (1990) 439.
5. A. MOROTTA, *J. Mater. Sci.* **16** (1981) 341.
6. A. A. LUDERER, *Rad. Res.* **94** (1983) 190.
7. Y. EBISAWA, *J. Ceram. Soc. Jpn* **99** (1991) 7.
8. Y. K. LEE and S. Y. CHOI, *J. Am. Ceram. Soc.* **79** (1996) 992.
9. M. B. VOLF, "Chemical Approach to Glass" (Elsevier, Amsterdam, 1984) p. 349.
10. P. F. JAMES, *Phys. Chem. Glasses* **15** (1972) 95.
11. M. AVRAMI, *J. Chem. Phys.* **7** (1939) 1103.
12. T. OZAWA, *Polymer* **12** (1971) 150.
13. H. E. KISSINGER, *Anal. Chem.* **29** (1957) 1702.
14. K. MATUSITA, *J. Mater. Sci.* **10** (1975) 961.
15. K. MATUSITA and S. SAKKA, *Phys. Chem. Glasses* **20** (1979) 81.
16. *Idem*, *J. Non-Cryst. Solids* **38–39** (1980) 741.
17. K. MATUSITA, *J. Mater. Sci.* **19** (1984) 291.
18. K. MATUSITA and KOMATSU, *Thermochim. Acta* **88** (1985) 283.
19. D. W. HENDERSON, *J. Non-Cryst. Solids* **30** (1979) 301.
20. H. YINNON, *ibid.* **54** (1983) 253.
21. M. MATSUURA and K. SUZUKI, *J. Mater. Sci.* **14** (1979) 395.
22. C. S. RAY, *J. Am. Ceram. Soc.* **74** (1991) 60.
23. X. J. XU, *ibid.* **74** (1991) 909.

Received 6 February  
and accepted 24 April 1994